

Stratospheric Influence on the Composition of the Mid- and Upper-Troposphere over North America sampled by the NASA DC-8 during INTEX A

Jack E. Dibb, Eric Scheuer, Robert Talbot

Climate Change Research Center, Institute for the Study of Earth, Oceans and Space
University of New Hampshire, Durham, NH

Melody Avery, ???
NASA Langley Research Center

Corresponding Author JED:
ph 603 862 3062, fax 603 862 2123, jack.dibb@unh.edu

30 June, 2006

Submitted to the JGR special section on INTEX A

ABSTRACT

A comprehensive atmospheric chemistry payload was deployed on NASA's DC-8 airborne laboratory for the INTEX A campaign in July and August, 2004. In-situ and remote measurements from the DC-8 were made to further understanding of the magnitude and distribution of anthropogenic emissions in North America, the processes exporting these emissions from the continental boundary layer, and the transformations they underwent as they were transported downwind to eastern North America and the Atlantic Ocean. We present the vertical and geographic distributions, and relationships between, ^7Be , O_3 , and HNO_3 in the INTEX A data set. Our objective is to identify stratospherically impacted air masses in the upper troposphere, and to estimate their influence on the composition of the upper troposphere, since unrecognized stratospheric influence may confound efforts to understand the fate of surface emissions lofted to the upper troposphere. Beryllium-7 and the HNO_3/O_3 ratio identify similar distinct stratospheric and tropospheric populations in the upper troposphere. Stratospherically impacted air was most common over the north eastern portion of the INTEX A study area. Estimates of the impact of stratospheric contributions on the upper tropospheric

budgets of O₃ and HNO₃ based on ⁷Be suggest that the stratosphere was the major source of both gases above 6 km. Using the HNO₃/O₃ ratio to filter out stratospheric influence suggest that the stratospheric source was important for HNO₃ (but much weaker than implied by ⁷Be) and minor for O₃. We investigate possible causes for these divergent results, but conclude that available data does not allow us to constrain the impact of the stratosphere on upper tropospheric composition in the INTEX A domain with useful precision using these tracers.

INTRODUCTION

The Intercontinental Chemical Transport Experiment, Phase A (INTEX A) was the NASA Tropospheric Chemistry Program's contribution to the International Consortium for Atmospheric Research on Transport and Transformation (ICARTT) intensive campaign in summer 2004. The overall campaign involved many different research assets deployed to sample the troposphere above North America and the North Atlantic to improve understanding of the magnitude, transformations, and fate of anthropogenic emissions from North America. INTEX had multiple science objectives of particular interest to NASA, in addition to those specific to ICARTT, these are detailed by *Singh et al.* [this issue a]. This overview of INTEX also provides specific objectives of each sortie that was flown, and describes the payload on board the DC-8 airborne laboratory for this mission.

One of the shared objectives of INTEX A and ICARTT 2004 was improved understanding of the export of anthropogenic and natural emissions from the North American boundary layer into the free troposphere, and subsequent transport over the North Atlantic and onto Europe. Very long-range transport of surface-based emissions is often facilitated if they are lofted into the upper troposphere where winds are usually stronger. Several companion papers discuss the evidence for significant vertical transport of North American emissions out of the boundary layer and lower troposphere by numerous convective storms over the continent during the campaign [e.g., *Bertram et al.*, 2006; *Cooper et al.*, this issue]. Polluted boundary layer air can be modified by loss of soluble components in wet convection, the addition of NO_x from lightning in the convective systems, and rapid photochemical processing within the upper troposphere.

An additional factor complicating efforts to understand the transformations and fate of anthropogenic emissions that reach the upper troposphere is mixing with stratospherically influenced air, which has enhanced mixing ratios of O₃ and HNO₃, two trace gases that are pollutants of concern in the lower troposphere. *Browell et al.* [this issue] identify and tabulate airmasses with stratospheric influence, determined by UV-DIAL, above and below the DC-8 on all INTEX A flights and *Avery et al.* [this issue] characterize the dynamical processes responsible for bringing stratospheric air into the troposphere in the INTEX A study region. While it is generally possible to recognize upper tropospheric air with a large stratospheric influence (and filter these data point out of some analyses, or track them as a special class of upper tropospheric air masses, e.g., *Singh et al.*, [this issue b]), there are often many more upper tropospheric air masses with weak stratospheric characteristics that are more difficult to identify.

In this paper we use the distributions of ⁷Be (a cosmogenic radionuclide formed mainly in the stratosphere), HNO₃, and O₃, and their inter-relationships, to: 1) identify air masses with both strong and weak stratospheric influences in the upper troposphere (above 6 km), and 2) attempt to constrain the impact of stratosphere to troposphere exchange on the upper tropospheric budgets of O₃ and HNO₃ above North America during INTEX A.

METHODS

The NASA DC-8 flew 18 science missions during INTEX A, starting and ending at NASA, Dryden. Two field bases were utilized, Middle America, just east of St. Louis, MO, and Pease Trade Port, in Portsmouth, NH. Local flights from Middle America were mainly over continental North America, but did extend to the Gulf of Mexico. Sorties from Pease covered much of the eastern US, but emphasized areas over extreme eastern Canada and the North Atlantic where chemical transport models indicated much of the export of North American emissions was occurring (see *Singh et al.*, [this issue a]).

In situ measurements of HNO₃ and O₃ were made on board the DC-8 by mist chamber/ion chromatography (MC/IC) and chemiluminescence (CL), respectively. The HNO₃ and O₃ systems have extensive track records in previous airborne campaigns on the DC-8 and other platforms. The automated MC/IC system was described by *Scheuer et al.* [2003], continued improvements to the IC analytical system allowed us to use a

sample integration time of 106 seconds throughout INTEX A. The FASTOZ CL instrument flown on recent DC-8 campaigns is described in *Avery et al.* [2006], O₃ measurements are reported at one second intervals. This paper relies on a merged data set produced at NASA Langley, wherein the faster O₃ measurements are averaged over the MC sample collection interval.

The activity of ⁷Be in bulk aerosol samples captured on glass fiber filters was determined by gamma spectroscopy, as described in *Dibb et al.* [1996]. We used the dual inlet aerosol probe described by *McNaughton et al.* [2006] and *Dibb et al.* [2003a] to expose simultaneous filter samples for the radionuclide tracers and for soluble ions. The aerosol-associated ion data is discussed by *Clarke et al.* [this issue], *Tang et al.* [this issue] and *Thornhill et al.* [this issue], this paper uses ⁷Be as an indicator of stratospheric influence.

Aerosol samples are collected only on level flight legs, so that sample flow rate can be adjusted to maintain isokinetic flow through the inlet nozzle. Filters were exposed for less than 5 minute intervals below 3 km pressure altitude, but integration time increased at higher altitudes. The overall average filter exposure interval was 7.1 minutes (range 2 – 27 minutes) during INTEX A, increasing to 11.1 minutes (range 5 – 27) above 6 km. Because one of the INTEX A objectives was to profile the entire troposphere above and downwind of North America [*Singh et al.*, this issue a], a large portion of each flight was spent climbing and descending (e.g., not sampling aerosols) (Figure 1). As a result, 45% of the MC sampling intervals do not have corresponding data on filter-collected aerosols. In the upper troposphere (> 6 km) the fraction of MC sampling time without ⁷Be data decreases to 27%, however, the average filter sample overlaps with approximately 6 MC samples. Rather than averaging the HNO₃, O₃, and NO₂ mixing ratios over the filter integration times, we repeat the ⁷Be activity within the corresponding MC sample intervals for subsequent analysis of the relationships between ⁷Be and the trace gases.

RESULTS

Beryllium-7 as Stratospheric Tracer.

Profiles of ^7Be and O_3 show gradual increases with altitude, and numerous large enhancements in individual samples above 6 km (Figure 2). *Avery et al.* [this issue] examine several of the DC-8 encounters with stratospheric air below the tropopause during INTEX A, and find that the cross-tropopause exchange had occurred both within the INTEX A region, as well as upwind, in different cases. They show that the subtropical jet largely determined the location of stratosphere-to-troposphere exchange (STE) impacting the troposphere above North America during INTEX A. The steady increase with altitude is consistent with STE constituting an important source of both ^7Be and O_3 in the upper troposphere (UT) over North America during INTEX A. Very large enhancements in both species at the highest altitudes reflect penetration of the lower stratosphere or tropopause folds, but finding $^7\text{Be} \gg 1000 \text{ fci m}^{-3} \text{ STP}$ and $\text{O}_3 \gg 100 \text{ ppb}$ as low as 6 km is surprising. The samples with very low ^7Be and O_3 in the UT are also of note, as they reflect convective pumping of boundary layer air into the UT [see *Bertram et al.*, 2006].

Nitric acid mixing ratios peak in the polluted continental boundary layer, so, in the context of a profile through the altitude sampling range of the DC-8 during INTEX A, the UT looks relatively clean (Figure 2). However, the mean mixing ratios in the 5-8 km, and $> 8 \text{ km}$, altitude ranges (264 ppt and 232 ppt, respectively) are elevated in comparison to what we have observed in the UT on previous campaigns. For example, the mean HNO_3 mixing ratio above 6 km over the Pacific during PEM West B was 130 ppt (when 6 samples in a tropopause fold near Japan were excluded) [*Dibb et al.*, 1997]. During TRACE P the mean mixing ratio was 175 ppt of HNO_3 , in the same altitude bin over a similar North Pacific region [*Dibb et al.*, 2003b]. Most of the INTEX A MC samples above 6 km with HNO_3 in excess of 500 ppt also had elevated ($> 150 \text{ ppb}$) O_3 mixing ratios. Enhanced UT HNO_3 , correlated with elevated O_3 , would also be consistent with STE impacting the composition of the UT over North America during the INTEX A campaign. However, it is also possible for tropospheric photochemistry to produce both O_3 and HNO_3 [e.g., *Bertram et al.*, 2006], accounting for some of their

observed upper UT burdens, and making positive correlations between them an ambiguous indicator of stratospheric origin.

Relatively weak tropospheric production of ^7Be (globally 2/3 of production is in the stratosphere [Lal *et al.*, 1958]) and rapid removal of the aerosols it is associated with by precipitation scavenging prevent purely tropospheric activities from exceeding several 100 fCi m^{-3} . Kritiz *et al.* [1991] suggest that 500 fCi m^{-3} STP is a good estimate for UT ^7Be activity, but this includes a stratospheric contribution. In contrast, in the stratosphere the sinks of ^7Be are radioactive decay and STE, leading to lifetimes on the order of a year compared to about a month in the upper troposphere [e.g., Dibb *et al.*, 1994]. At 15 km altitude (close to the zone of maximum production) near 40° the steady state ^7Be activity has been estimated to be 8 pCi m^{-3} [Bhandari *et al.*, 1966], thus STE causes large, and unambiguous, enhancements in ^7Be below the tropopause. Correlations of other species with ^7Be in the troposphere can therefore be used to assess whether STE is also a significant source for them.

In the INTEX A data set O_3 is reasonably correlated with ^7Be when all samples are considered (Figure 3, solid line in upper panel). For HNO_3 there are clearly two separate populations, a tropospheric group with high HNO_3 but low ^7Be , and a stratospheric branch where they increase together. We selected $600 \text{ fCi } ^7\text{Be m}^{-3}$ STP as an admittedly arbitrary, but reasonable, threshold to define lower stratospheric and strongly STE impacted UT air masses in the INTEX A data set, and present the linear relation between O_3 and ^7Be in these “stratospheric” samples in the lower panel of Figure 3. Since the HNO_3 data shows there is clearly a distinct stratospheric and stratospherically impacted subset of the INTEX A data set, we also used the $600 \text{ fCi } ^7\text{Be m}^{-3}$ STP threshold to examine the $\text{O}_3 - ^7\text{Be}$ relationship in this group of samples with strong stratospheric influence. The linear regression of O_3 against $^7\text{Be} > 600 \text{ fCi m}^{-3}$ STP (shown as the dotted line in upper panel of Figure 3) has a 27% lower intercept and a 13% steeper slope than the fit to the entire data set. The fact that the two relationships are so similar reflects the dominant impact of the small number of samples with very strong stratospheric character, over the cloud of points with low ^7Be activity and low to moderate O_3 mixing ratios, on the regression.

If we assume that the regression lines in Figure 3 represent mixing lines between tropospheric air and a stratospheric source with constant, greatly enhanced, ^7Be , O_3 , and HNO_3 , we can use measured ^7Be to estimate the stratospheric mixing ratios of O_3 and HNO_3 in all INTEX A samples for which we have ^7Be data [e.g., *Dibb et al.*, 2000, 2003c]. An estimate of the tropospheric fraction of O_3 and HNO_3 in each sample can then be obtained by subtracting the calculated “stratospheric” mixing ratio from the actual measurement (i.e., $\text{Trop O}_3 = \text{Measured O}_3 - \text{estimated Strat O}_3$). Using the relationship for the full data set ($\text{Strat O}_3 = (0.039 \times ^7\text{Be}) + 50.1$, from the solid line in upper panel of Figure 3) yields a mean tropospheric O_3 mixing ratio of 8.8 ppb above 8 km, and -2.2 ppb between 5 and 8 km. If the regression using the $^7\text{Be} > 600 \text{ fCi m}^{-3}$ STP threshold is used (dotted line in upper panel of Figure 3), the estimated mean tropospheric O_3 is 8.6 and 17.7 ppb, respectively, in the same altitude bins.

Given observed mean O_3 mixing ratios of 91 and 71 ppb in these altitude bins, this analysis suggests that more than 90% of the O_3 above 8 km came from the stratosphere, and 75% to more than 100% of O_3 in the mid troposphere is also stratospherically derived. Parallel calculations for HNO_3 suggest an 88% contribution from the stratosphere above 8 km (28 ppt mean tropospheric HNO_3 compared to 232 ppt observed mean) and a 61% contribution in the 5 – 8 km range (104 ppt versus 264 ppt). In contrast, using a filter to screen out UT samples with obvious stratospheric influence (all samples above 7 km with $\text{O}_3 > 120$ ppb and H_2O vapor < 100 ppm) results in mean mixing ratios of O_3 and HNO_3 above 8 km of 79 ppb and 203 ppt, respectively [*Singh et al.*, this issue b]. This approach suggests that STE makes about a 13% contribution to the mean mixing ratios of both gases in the INTEX upper UT. However, it excludes, by definition, the possibility of any stratospheric component in an air mass with less than 120 ppb O_3 , and would consider the samples with clear stratospheric signatures of O_3 and ^7Be between 6 and 7 km (Figure 2) to be tropospheric. The large number of samples with O_3 mixing ratios in the ~ 60 to 120 ppb range with 500 to 1000 ppt of HNO_3 (Figure 4) create ambiguity when using threshold values of any tracer, or combination of tracers, to screen out stratospheric influence in the troposphere.

Pierce et al. [this issue] use the RAQMS 3-D chemical transport model, with chemical data assimilation, to assess the tropospheric budgets of O_3 and HNO_3 over

North America during INTEX A. They suggest that the net cross-tropopause flux of both gases within the CONUS domain is actually upward into the lower stratosphere.

However, they also find that much of the UT O₃ and HNO₃ advected into the INTEX A domain across the western border within the UT, after having been injected into the UT by STE upwind over the Pacific. This may be consistent with the ⁷Be-based estimates of very strong stratospheric influence on the UT during INTEX A, since the measured ⁷Be activity provides no insight into where STE may have occurred. Analysis of ozone sondes launched in support of the ICARTT campaign also lend support to the assertion of significant stratospheric influence in the North American troposphere during INTEX A [Thompson *et al.*, this issue], as does the analysis of O₃ curtains derived from the UV-DIAL system on the DC-8 [Browell *et al.*, this issue].

The estimates of stratospheric influence on the composition of the upper troposphere over North America from ⁷Be would appear to preclude significant photochemical production of O₃ and HNO₃ above 6 km during INTEX A. This assertion is at odds with several model studies of the INTEX A data set. Bertram *et al.* [2006] simulate rapid production of both O₃ (up to 7.5 ppb d⁻¹ for the first two days) and HNO₃ in air masses recently convected into the UT. They also estimate that 40% of the air masses sampled by the DC-8 between 7.5 and 11.5 km had been convectively uplifted within less than two days before sampling. It should be noted that the recently convected air masses in the UT identified by elevated NO_x/HNO₃ (or NO₂/HNO₃) start with low mixing ratios of O₃ (reflecting origin in the boundary layer) and HNO₃ (which is effectively scavenged in the convective systems). Cooper *et al.* [this issue] also suggest that convected boundary layer NO_x, and NO_x from lightning in the convective systems, make a major contribution to O₃ enhancements observed in the UT during INTEX A, particularly over the southern regions. Constrained box model calculations find net production of O₃ across the INTEX A UT as well [Crawford *et al.*, this issue]. The RAQMS simulations discussed above also find significant net O₃ production in the troposphere, but mainly in the first few weeks of INTEX A, with net loss apparent in the tropospheric column after the end of July [Pierce *et al.*, this issue].

It should be borne in mind that requiring observations of ⁷Be above detection limit for our analysis reduces the data sets from 1464 samples to 828 samples above 8

km, and from 1075 to 395 samples between 5 and 8 km. We also acknowledge that the estimates of stratospheric mixing ratios have large uncertainty due to the significant scatter about the regression (Figure 3). Estimating the tropospheric residual has additional uncertainty due simply to the precision of the multiple measurements needed to make the calculation. We will return to these, and other, issues impacting this approach to estimating stratospheric influence on the troposphere in the discussion.

HNO₃/O₃ as a Stratospheric Tracer.

Given that O₃ and HNO₃ are each correlated with ⁷Be in the upper troposphere, a positive correlation between O₃ and HNO₃ would be expected. A scatter plot reveals that there are two distinct populations in the complete INTEX A data set (Figure 4, upper panel). Samples with > 1 ppb HNO₃ but O₃ generally < 100 ppb define the polluted boundary layer and lower troposphere, with a smaller stratospherically impacted group of samples defined by a much shallower HNO₃/O₃ slope, but higher O₃ mixing ratios. The INTEX A data points are plotted on top of the results we obtained from the DC-8 during the Polar Aura Validation Experiment (PAVE) in January, 2005 [Dibb *et al.*, 2006]. The DC-8 was also based at Pease for PAVE and conducted 6 sorties north into the Arctic; the vast majority of sampling was conducted in the lower stratosphere. A very small tropospheric subset of PAVE results is present, but not visible, under the INTEX A data. The INTEX A stratospherically influenced samples fall along the bottom of the distribution of PAVE stratospheric samples. During PAVE, the HNO₃/O₃ ratio was always near 3.5 ppt/ppb in the stratosphere, except when perturbed by renitrification at DC-8 flight levels [Dibb *et al.*, 2006]. The PAVE stratospheric ratio is also shown in the lower panel of Figure 4, superimposed on all INTEX A samples collected above 6 km. The 3.5 ppt/ppb slope is a reasonable depiction of the INTEX A stratospherically impacted population, if the line is extrapolated to 40 ppb O₃ at 0 ppt HNO₃.

We observed that the HNO₃/O₃ ratio above 6 km during INTEX A was often near the PAVE stratospheric value of 3.5 ppt/ppb, except when HNO₃ was depressed in recently convected air masses, as indicated by simultaneous enhancements of NO₂/HNO₃ and decreases in HNO₃/O₃ (Figure 5), and more rarely when HNO₃ was enhanced in biomass burning plumes (not observed during the example Flight #11 shown in Figure 5).

Scatter plots of HNO₃ and O₃ against the HNO₃/O₃ ratio also show two subpopulations in the INTEX A UT data set, with the stratospherically impacted group identified in Figures 3 and 4 largely restricted to values of HNO₃/O₃ between 2.0 and 4.0 (Figure 6). This suggests that the HNO₃/O₃ ratio may be complementary to ⁷Be as a tracer of stratospheric influence in the UT. If true, this ratio is available at the 106 second MC sample resolution throughout the UT.

All INTEX A UT (>6 km) samples were divided into 4 geographic bins: west of 80 W and south of 41 N (SW), west of 80 W and north of 41 N (NW), east of 80 W and south of 41 N (SE), and east of 80 W and north of 41 N (NE). The spatial bins were also divided into 3 upper tropospheric altitude bins and the fraction of all MC sampling intervals with HNO₃/O₃ near the PAVE stratospheric ratio (2.0– 4.0 ppt/ppb (Figure 6)) were compiled (Table 1). The fraction of UT samples identified as stratospherically impacted by this ratio was highest in the NE bin, followed by the SW. One might have expected the NW bin to also show frequent stratospheric influence, reflecting the lower tropopause at higher latitudes. *Browell et al.* [this issue] also find more stratospheric influence in the troposphere in the north east portion of the INTEX A study area. Enhanced STE over the NE bin likely reflects regionally lower tropopause heights associated with the persistent trough over eastern North America during INTEX A that largely overlapped the period when the DC-8 was based in New Hampshire [*Fuelberg et al.*, this issue].

In the NE and SW regions, the frequency of samples with $2.0 < \text{HNO}_3/\text{O}_3 < 4.0$ is highest in the top altitude range and decreases downward. This is consistent with STE being the source of the air masses with this proposed characteristic ratio. The decreasing trend in apparent stratospheric influence as altitude increases seen in the NW and SE regions is less easy to understand, especially the high fractions in the 6 – 8 km range (Table 1). It may be that many of the low altitude samples with the “stratospheric” HNO₃/O₃ signature in these regions come from the intersection of the two arms of the distributions in Figure 6.

If the HNO₃/O₃ ratio is reflecting stratospheric influence, weighting the percentages in Table 1 by the number of samples collected in each of the bins suggests that 34% of air masses above 8 km across the entire INTEX A study region were

impacted by STE. *Fuelberg et al.* [this issue] find that 27% of back trajectories from the DC-8 flight tracks at all altitudes during INTEX A encountered the stratosphere within the previous 10 days. Presumably that percentage is higher at higher altitudes, so our estimate of 34% of samples above 8 km having stratospheric influence seems reasonable, and may even be conservative. If this is combined with the *Bertram et al.* [2006] estimate that 40% of air sampled between 7.5 and 11.5 km was lifted from the boundary layer within two days, the UT would seem to be dominated by air mixing in from other regions of the atmosphere.

We are suggesting that the HNO_3/O_3 ratio identifies samples that retain a stratospheric signature, but do not necessarily have mixing ratios characteristic of the stratosphere. Similarly, recently convected air masses start with compositions reflecting their boundary layer origin (except that soluble gases and particles can be depleted by precipitation scavenging enroute to the upper troposphere), but these are quickly modified by photochemical processes *Bertram et al.* [2006]. Hence, it is clearly an oversimplification to expect that the composition of the upper troposphere should be a simple mixture of the three components; boundary layer air, lower stratosphere, and background upper troposphere (if such a component can be defined).

In a first order attempt to quantify the impact of stratospheric and convective inputs on UT composition we have filtered two groups of samples out of the INTEX A UT data set. The stratospherically impacted subset is defined as above, $2.0 < \text{HNO}_3/\text{O}_3 < 4.0$. To select recently convected airmasses we used $\text{NO}_2/\text{HNO}_3 > 1.0$, which is a more restrictive criterion than that used by *Bertram et al.* [2006] ($\text{NO}_x/\text{HNO}_3 > 1.0$). These two filters identify two nearly distinct populations, just 37 of the 2251 samples above 6 km fall into both groups, most of these are in the SW region.

Mean HNO_3 mixing ratios above 6 km increase in nearly all of the spatial/altitude bins if recently convected air masses are excluded (Figure 7). The largest differences are seen in the > 10 km bins in all regions, with more than 17% increases in the means (up to 31% in NE). The impact of convection is also relatively strong from 8 – 10 km in the SE and NE regions, where mean HNO_3 increases 11 and 12%, respectively, without the convective samples. Excluding the stratospheric samples depresses mean HNO_3 mixing ratios in 6 of the 8 bins above 8 km (Figure 7). The decrease only exceeds 10% in the

SW > 10 km, SE 8 – 10 km, and two highest NE bins. It should be noted that the means above 8 km in NE decrease by more than 30%, with nearly equal impacts seen in the 8 – 10 and > 10 km ranges. The overall decrease above 8 km is modest compared to the 88% contribution from the stratosphere estimated from HNO₃ versus ⁷Be. At 6 – 8 km in all regions removing the samples identified as stratospherically impacted actually causes the HNO₃ mean to increase modestly, contrasting even more starkly with the estimate from ⁷Be that STE contributed 61% of the HNO₃ in the 5-8 km range over the INTEX A domain.

Results for O₃ are even more discordant with the ⁷Be based estimates. Excluding “stratospheric” samples from the UT data set decreases the mean by 15% from 8 – 10 km in the SE and NE bins, and by 20% above 10 km in NE (Figure 8). In 4 of the 5 other bins above 8 km the mean O₃ actually increases slightly when the stratospherically influenced samples are excluded (and the decrease in the SW region above 10 km is just over 2%). At 6 – 8 km all regions show small decreases, but the largest is < 6% (NE region). Recall that the ⁷Be-based approach attributed more than 90% of the O₃ above 8 km to STE. The impact of recently convected air masses on the O₃ content of the upper troposphere is also suggested to be very modest by this analysis (Figure 8). In 3 of the highest altitude bins, mean O₃ increases by ~ 5%, reaching a maximum of 15% in the NE, when the convective samples are ignored. In all other bins the means increase by < 4% (< 2% in 7 of the 8) when filtered to exclude very recent convection (Figure 8).

Excluding the samples identified as stratospheric by the HNO₃/O₃ ratio yields mean mixing ratios of 194 ppt HNO₃ and 82 ppb O₃ across the entire INTEX A study area above 8 km, corresponding to 16 and 10% reductions compared to the overall mean mixing ratios of HNO₃ and O₃ in this altitude range. Stratospheric influence above 8 km is thus estimated to be 3% larger for HNO₃ and 3% smaller for O₃ than was the case for the O₃ and H₂O vapor filter used by *Singh et al.* [this issue b] to remove stratospherically impacted samples from the UT data set. As noted earlier, when comparing this filter to the ⁷Be based estimates of stratospheric influence, the 120 ppb O₃ and 100 ppm H₂O criteria appear to classify significant numbers of sample with stratospheric influence as purely tropospheric and would thus be a lower bound to stratospheric influence on the composition of the UT.

DISCUSSION

There is no doubt that the DC-8 flew into the lower stratosphere on some flights, and also penetrated tropopause folds, during INTEX A (see Figures 2-4). It is also very certain that the UT contained airmasses that had been influenced by STE relatively recently, resulting in enhancements of a suite of trace gases and tracers that are greatly enriched in the stratosphere compared to the troposphere (e.g., O_3 , HNO_3 , and 7Be). Air in the lower stratosphere also has markedly lower than tropospheric concentrations of a suite of gases (e.g., H_2O , CO , CH_4 , N_2O), so depletions in these gases in the UT can serve as additional tracers of STE. We examined the relationships between water vapor and the stratospheric tracers 7Be and HNO_3/O_3 in the INTEX A data set, but found nothing that would explain why 7Be implies a dominant stratospheric impact throughout the UT during INTEX A, while HNO_3/O_3 suggested a minor role for STE, particularly for O_3 . Unfortunately, the availability of CO and CH_4 data is limited and no measurements of N_2O were made during INTEX A due to instrument problems.

Beryllium-7 is not photochemically produced (unlike O_3 and HNO_3), hence it has long been used as a tracer to identify stratospheric influence in the troposphere, and has less frequently been used to estimate the magnitude of such influence on the composition of the troposphere. In airborne campaigns 7Be has been used for both purposes [e.g., *Kritz et al.*, 1991; *Dibb et al.*, 2000, 2003c], but the low time resolution, and lack of data on ascending and descending flight legs, imposed by filter based sampling and analytical constraints, have been limitations. In this paper we attempt to use 7Be to quantify the impact of STE on the concentrations of two important trace gases in the UT, and explore the suggestion that the lower stratosphere may have a narrow characteristic range of the ratio HNO_3/O_3 , such that the ratio could be a complementary tracer of stratospheric influence in the troposphere, available at much higher temporal resolution.

Enhanced 7Be activity and values of the HNO_3/O_3 ratio between 2.0 and 4.0 both identify a distinct subset of observations in the UT that have correlated enhancements in O_3 and HNO_3 consistent with stratospheric origin (Figures 3 and 6). In fact, the ratio (Figure 6) more clearly discriminates the stratospherically influenced O_3 observations that are apparent in the HNO_3 versus O_3 scatter plot (Figure 4) than does 7Be activity

(Figure 3). Both approaches suggest that a significant number of samples in the UT during INTEX A had stratospheric influence. However, when they are used to estimate how much of the UT burden of HNO₃ and O₃ during INTEX A resulted from STE, the results are widely divergent for HNO₃, and even more so for O₃ (Figures 7 and 8). Using correlations with ⁷Be to estimate the stratospheric fraction of O₃ and HNO₃ in the UT suggests that STE is an overwhelmingly dominant influence, while the HNO₃/O₃ filter suggests a minor contribution from the stratosphere. It is unclear which is closer to the truth.

It may be that the HNO₃/O₃ ratio loses discriminatory power as the fraction of stratospherically derived air in a sample diminishes. In the INTEX A UT data set the range of values in HNO₃/O₃ that capture the clearly stratospheric samples also include many samples that could be in the tropospheric population, with HNO₃ < 500 ppt and O₃ < 120 ppb) (Figure 6). In addition, processing in the troposphere (precipitation scavenging and photochemistry) will likely change the HNO₃/O₃ ratio over time.

The poor temporal and vertical coverage of ⁷Be data obtained in airborne campaigns is not likely to cause systematic over estimation of stratospheric influence. The technique used here assumes that all of the ⁷Be measured in the troposphere originated in the stratosphere, which is not strictly true. Subtracting a tropospheric fraction from measured ⁷Be would result in lower estimates of stratospheric influence, but it is not clear how to determine the partitioning between the two sources of ⁷Be. Likewise, we could require a minimum threshold of measured ⁷Be before using a data point to estimate the stratospheric contributions to simultaneously measured O₃ or HNO₃, but establishing that threshold would be arbitrary. Another possible flaw in the ⁷Be technique applied here (and previously, e.g., *Dibb et al.*, 2000, 2003c) is in the treatment of the intercept derived from the regression analysis (Figure 3). It has been suggested that the intercept should be interpreted as the tropospheric background into which the stratospheric contribution is mixing (Daniel Jacob, personal communication, August, 2004). In this conceptual model, the stratospheric component of O₃ or HNO₃ would be given simply by measured ⁷Be x the slope found by regression, and the tropospheric residual would obviously be larger than the estimates presented in Figures 7 and 8.

We have applied this modified ^7Be approach to the INTEX A data set, to see if it would reconcile the different estimates of stratospheric influence on the composition of the UT based on HNO_3/O_3 and ^7Be . Except for HNO_3 in the NE region above 8 km the two approaches are still divergent, with ^7Be suggesting a much stronger impact from STE (Figures 9 and 10). The estimated stratospheric contribution to UT O_3 above 8 km across the entire INTEX A region, based on this weaker link to ^7Be , is 42% of the total, compared to the 10% contribution inferred from the HNO_3/O_3 ratio as a filter approach. For HNO_3 the comparison is 47% stratospheric contribution from ^7Be and 16% using the HNO_3/O_3 ratio.

CONCLUSIONS

The altitude distributions of ^7Be , HNO_3 , and O_3 above the INTEX A study region, and correlations between these species in the UT, provide evidence that stratospheric air was sampled occasionally during the mission. In addition, these three tracers suggest that air masses with stratospheric influence were encountered frequently above 6 km altitude, with distinct tropospheric and stratospherically influenced populations revealed by two, relatively compact, branches with different slopes in scatter plots of HNO_3 versus O_3 and HNO_3 versus ^7Be . The slope of the stratospherically impacted branch of the $\text{HNO}_3 - \text{O}_3$ relationship in the UT during INTEX A was similar to that found in the lower stratosphere above northeastern North America during PAVE, suggesting that HNO_3/O_3 might serve as an additional tracer of stratospheric influence in the troposphere.

We have used the established ^7Be tracer, and HNO_3/O_3 as a proposed new tracer, to identify INTEX A samples in the UT with stratospheric influence, and to attempt to quantify the impact of STE on the mixing ratios of O_3 and HNO_3 in the UT. The two approaches both suggest that stratospherically impacted airmasses were frequently encountered, and that they were found most frequently in the northeastern portion of the INTEX A study region, in accord with other analyses of the INTEX A and ICARTT data sets.

Estimates of the fraction of HNO_3 and O_3 in the UT that was derived from the stratosphere were made by correlations to ^7Be , and by using the HNO_3/O_3 ratio as a filter to exclude stratospherically impacted air masses. The approach using ^7Be suggests that

STE was the dominant source of both gases above 6 km altitude during the campaign, while the HNO_3/NO_2 filter indicates that STE is a significant (though not dominant) source of HNO_3 in the UT, but plays only a minor role in the UT O_3 budget. While the HNO_3/O_3 ratio does identify samples with strong (recent?) stratospheric influence, it appears to also select too many with little or no stratospheric influence, so that the subpopulation selected by this filter in the INTEX A data set has a tropospheric character. On the other hand, the O_3 and HNO_3 versus ^7Be relationships overestimate stratospheric influence by not considering the presence of a small, but unknown, tropospheric fraction of ^7Be in each sample. There is also uncertainty regarding whether the intercepts in the regression analyses should be included as part of the “stratospheric” HNO_3 and O_3 , or considered the tropospheric endmember into which the stratospheric contribution is mixed. The latter approach yields smaller estimates of impact of STE on the UT, but even these estimates suggest that STE was a dominant factor in the budgets of UT HNO_3 and O_3 during INTEX A. It is likely that the true impact of STE on UT HNO_3 and O_3 lies between these two ^7Be -based estimates. Measurements of additional stratospheric tracers, that were not available during INTEX A, were made during INTEX phase B in spring 2006; these may provide insight into the discrepancies between the different estimates of stratospheric influence on the composition of the UT described here.

REFERENCES CITED

- Avery, M. A., et al., FASTOZ: An accurate, fast-response in situ ozone measurement system for aircraft campaigns (2006), submitted to *J. Oceanic Atmos. Tech.*
- Avery, M. A., et al. (this issue), Impact of multi-scale dynamical processes and mixing on the chemical composition of the upper troposphere and lower stratosphere as observed and modeled during INTEX A, submitted to *J. Geophys. Res.*
- Bertram, T. H., A. E. Perring, P. J. Woolridge, R. C. Cohen, P. O. Wennberg, J. Dibb, A. Clarke, W. H. Brune, S. A. Vay, M. Avery, G. Sachse, J. H. Crawford, G. Huey, H. Fuelberg, B. G. Heikes, and A. Fried (2006), Chemical constraints on convective influence in the upper troposphere, submitted to *Science*.
- Bhandari, N., D. Lal, and Rama (1966), Stratospheric circulation studies based on natural and artificial radioactive tracer elements, *Tellus*, *18*, 391-405.
- Browell, E. V., M. A. Fenn, J. W. Hair, C. F. Butler, A. Notari, S. A. Kooi, S. Ismail, M. A. Avery, R. B. Pierce, and H. E. Fuelberg (this issue), Large-scale air mass characteristics observed during the summer over North America and Western Atlantic Ocean, submitted to *J. Geophys. Res.*
- Clarke, A. D., V. Kapustin, S. G. Howell, C. S. McNaughton, Y. Shinozuka, B. Anderson, and J. Dibb (this issue), Aerosol from biomass burning and regional pollution over North America during INTEX-NA: Humidity response and the wavelength dependence of scattering and absorption, submitted to *J. Geophys. Res.*
- Cooper, O. R., A. Stohl, M. Trainer, A. Thompson, J. C. Witte, S. J. Oltmans, B. J. Johnson, J. Merrill, J. L. Moody, G. Morris, D. Tarasick, G. Forbes, P. Nedelec, F. C. Fehsenfeld, J. Meagher, M. J. Newchurch, F. J. Schmidlin, S. Turquety, J. H. Crawford, K. E. Pickering, S. L. Baughcum, W. H. Brune, and C. C. Brown (this issue), Large upper tropospheric ozone enhancements above mid-latitude North America during summer: In situ evidence from the IONS and MOZAIC ozone monitoring network, submitted to *J. Geophys. Res.*
- Crawford, J., J. Olsen, G. Chen, W. Brune, A. Fried, B. Heikes, L. G. Huey, M. Avery, G. Sachse, G. Diskin, R. Cohen, and H. Singh (this issue), Summertime ozone production over North America during INTEX-A based on observed and modeled photochemistry, submitted to *J. Geophys. Res.*
- Dibb, J. E., L. D. Meeker, R. C. Finkel, J. R. Southon, M. W. Caffee, and L. A. Barrie (1994), Estimation of stratospheric input to the Arctic troposphere: ^7Be and ^{10}Be in aerosols at Alert; *J. Geophys. Res.*, *99*, 12,855-12,864.
- Dibb, J. E., R. W. Talbot, K. I. Klemm, G. L. Gregory, H. B. Singh, J.D. Bradshaw, and S. T. Sandholm (1996), Asian influence over the western north Pacific during the fall season: Inferences from lead 210, soluble ionic species, and ozone, *J. Geophys. Res.*, *101*, 1779-1792.
- Dibb, J. E., R. W. Talbot, B. L. Lefer, E. Scheuer, G. L. Gregory, E. V. Browell, J. D. Bradshaw, S.T. Sandholm, and H. B. Singh (1997), Distributions of beryllium 7 and lead 210 and soluble aerosol-associated ionic species over the western Pacific: PEM West B, February – March 1994, *J. Geophys. Res.*, *102*, 28,287-28,302.
- Dibb, J. E., R. W. Talbot and E. M. Scheuer (2000) Composition and distribution of aerosols over the North Atlantic during the Subsonic Assessment Ozone and Nitrogen Oxide Experiment (SONEX); *J. Geophys. Res.*, *105* 3709-3717.

- Dibb, J. E., R. W. Talbot, G. Seid, C. Jordan, E. Scheuer, E. Atlas, N. J. Blake, and D. R. Blake (2003a), Airborne sampling of aerosol particles: Comparison between surface sampling at Christmas Island and P-3 sampling during PEM Tropics B, *J. Geophys. Res.*, *107*, 8230, doi:10.1029/2001JD000408, 2002. [printed *108*(D2), 2003].
- Dibb, J. E., R. W. Talbot, E. M. Scheuer, G. Seid, M. A. Avery, and H. B. Singh (2003b), Aerosol chemical composition is Asian continental outflow during the TRACE-P campaign: Comparison with PEM West B, *J. Geophys. Res.*, *108*(D21), 8815, doi:10.1029/2002JD003111.
- Dibb, J. E., R. W. Talbot, E. Scheuer, G. Seid, L. J. DeBell, B.L. Lefer, and B. A. Ridley (2003c), Stratospheric influence on the northern North American free troposphere during TOPSE: ⁷Be as a stratospheric tracer, *J. Geophys. Res.*, *108* (D4), 8363, doi:10.1029/2001JD001347.
- Dibb, J. E., E. Scheuer, M. Avery, J. Plant, and G. Sachse (2006), In situ evidence for renitrification in the Arctic lower stratosphere during the polar aura validation experiment (PAVE), *Geophys. Res. Lett.*, in press.
- Fuelberg, H. E., M. J. Porter, C. M. Kiley, D. Morse (this issue), Meteorological conditions and anomalies during INTEX-NA, submitted to *J. Geophys. Res.*
- Kritz, M. A., S. W. Rosner, E. F. Danielsen, and H. B. Selkirk (1991), Air mass origins and and troposphere-to-stratosphere exchange associated with midlatitude cyclogenesis and tropopause folding inferred from ⁷Be measurements, *J. Geophys. Res.*, *96*, 17,405-17,414.
- Lal, D., P. K. Malhotra, and B. Peters (1958) On the production of radioisotopes in the atmosphere by cosmic radiation and their application to meteorology, *J. Atmos. Terr. Phys.*, *12*, 306-328.
- McNaughton, C. S., L. Thornhill, A. D. Clarke, S. G. Howell, M. Pinkerton, B. Anderson, E. Winstead, C. Hudgins, H. Maring, J. E. Dibb, and E. Scheuer (2006), Results from the DC-8 inlet characterization experiment (DICE): Airborne versus surface sampling of mineral dust and sea salt aerosols, submitted to *Aerosol Sci. Tech.*
- Pierce, R. B., T. K. Schaak, J. Al-Saadi, T. D. Fairlie, C. Kittaka, G. Lingenfelter, M. Natarajan, J. Olson, A. Soja, T. H. Zapotocny, A. Lenzen, D. R., Johnson, M. Avery, G. Sachse, A. Thompson, R. Cohen, J. Dibb, J. Crawford, D. Rault, R. Martin, J. Szykman, and J. Fishman (this issue), Chemical data assimilation estimates of continental US ozone and nitrogen budgets during INTEX-A, submitted to *J. Geophys. Res.*
- Scheuer, E., R. W. Talbot, J. E. Dibb, G. K. Seid, L. DeBell, and B. Lefer (2003), Seasonal distribution of fine aerosol sulfate in the North American Arctic during TOPSE, *J. Geophys. Res.*, *108*(D4), 8370, doi: 10.1029/2001JD001364.
- Singh, H. B., W. Brune, J. Crawford, and D. Jacob (2006), Overview of the summer 2004 Intercontinental Chemical Transport Experiment-North America (INTEX-A), submitted to *J. Geophys. Res.*
- Singh, H. B., L. Salas, D. Herlth, R. Kolyer, E. Czech, M. Avery, J. H. Crawford, R. B. Pierce, G. W. Sachse, D. R. Blake, R. C. Cohen, J. Dibb, G. Huey, R. C. Hudman, S. Turquety, L. K. Emmons, F. Flocke, Y. Tang, G. R. Carmichael, and L. W. Horowitz (this issue), Reactive nitrogen distribution and partitioning in the North American troposphere and lowermost stratosphere, submitted to *J. Geophys. Res.*

- Tang, Y., G. R. Carmichael, N. Thongboonchoo, T. Chai, L. W. Horowitz, R. B. Pierce, J. A. Al-Saadi, G. Pfister, J. M. Vukovich, M. A. Avery, G. W. Sachse, T. B. Ryerson, J. S. Holloway, E. L. Atlas, F. M. Flocke, R. J. Weber, L. G. Huey, J. E. Dibb, D. G. Streets, and W. H. Brune (2006), The influence of lateral and top boundary conditions on regional air quality prediction: A multi-scale study coupling regional and global chemical transport models, submitted to *J. Geophys. Res.*
- Thompson, A. M., J. B. Stone, J. C. Witte, R. B. Pierce, R. B. Chatfield, S. J. Oltmans, O. R. Cooper, B. F. Taubman, B. J. Johnson, E. Joseph, T. L. Kucsera, J. T. Merrill, G. A. Morris, M. J. Newchurch, F. J. Schmidlin, D. W. Tarasick, and V. Thouret (this issue), Stratospheric contributions to tropospheric ozone profiles in eastern North America, July-August 2004 (IONS): A typical “Spring-like Summer?”, submitted to *J. Geophys. Res.*
- Thornhill, K. L., B. E. Anderson, G. Chen, E. L. Winstead, A. D. Clarke, Y. Shinozuka, C. McNaughton, J. Dibb, E. Scheuer, C. Jordan, D. R. Blake, G. Sachse, A. Fried, G. Huey, R. Cohen, and P. Wennberg (2006), The impact of continental outflow on chemical and aerosol distributions off the Northeast U. S. coast during INTEX-NA, submitted to *J. Geophys. Res.*
- Thornton, J. A., et al. (2000), Atmospheric NO₂: In situ laser-induced fluorescence detection at parts per trillion mixing ratios, *Analytic. Chem*, 72,528-539.

Table 1. Percentage of mist chamber sampling intervals with HNO₃/O₃ ratios characteristic of the lower stratosphere (2.0 – 4.0 ppt/ppb).

Press. Alt. (km)	Spatial Region			
	South West	North West	South East	North East
6 – 12	34.8 (660) ¹	30.4 (319)	30.5 (390)	42.4 (882)
10 – 12	37.4 (230)	10.8 (83)	17.4 (92)	45.4 (152)
8 – 10	34.6 (191)	28.7 (136)	27.5 (171)	42.5 (409)
6 – 8	32.6 (239)	49.0 (100)	44.1 (127)	40.8 (321)

¹ (Total number of samples collected in each bin in brackets)

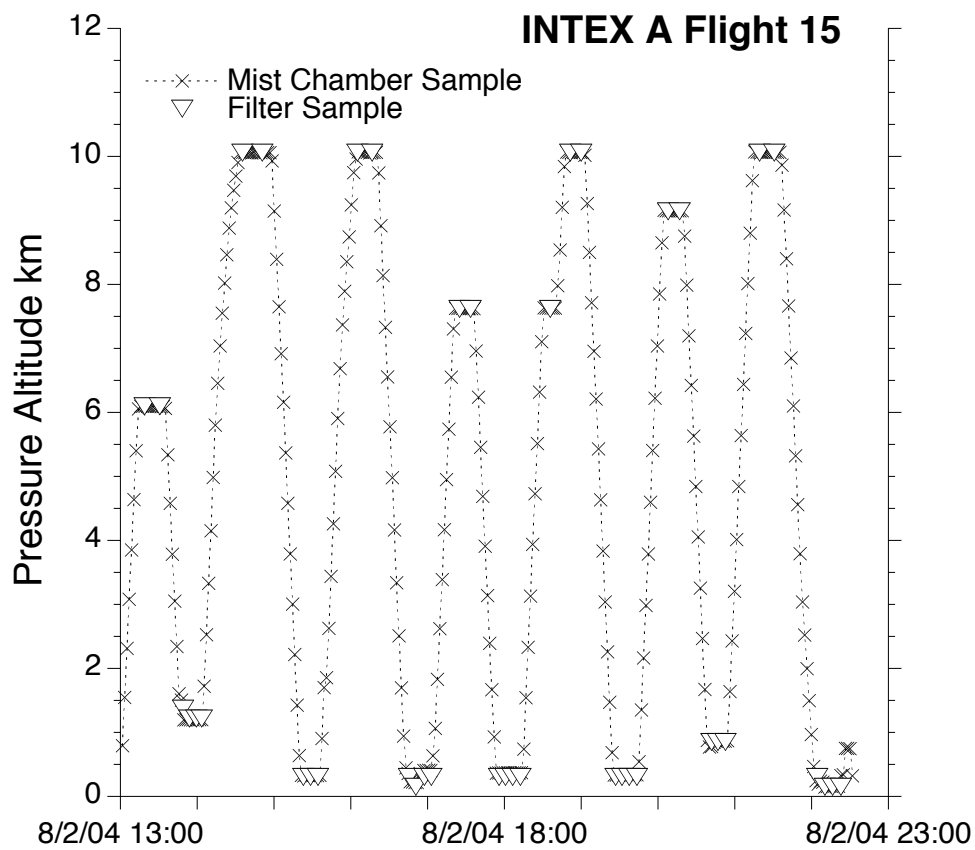


Figure 1. Example of the distribution of mistchamber and filter samples over time and altitude on a typical INTEX A flight.

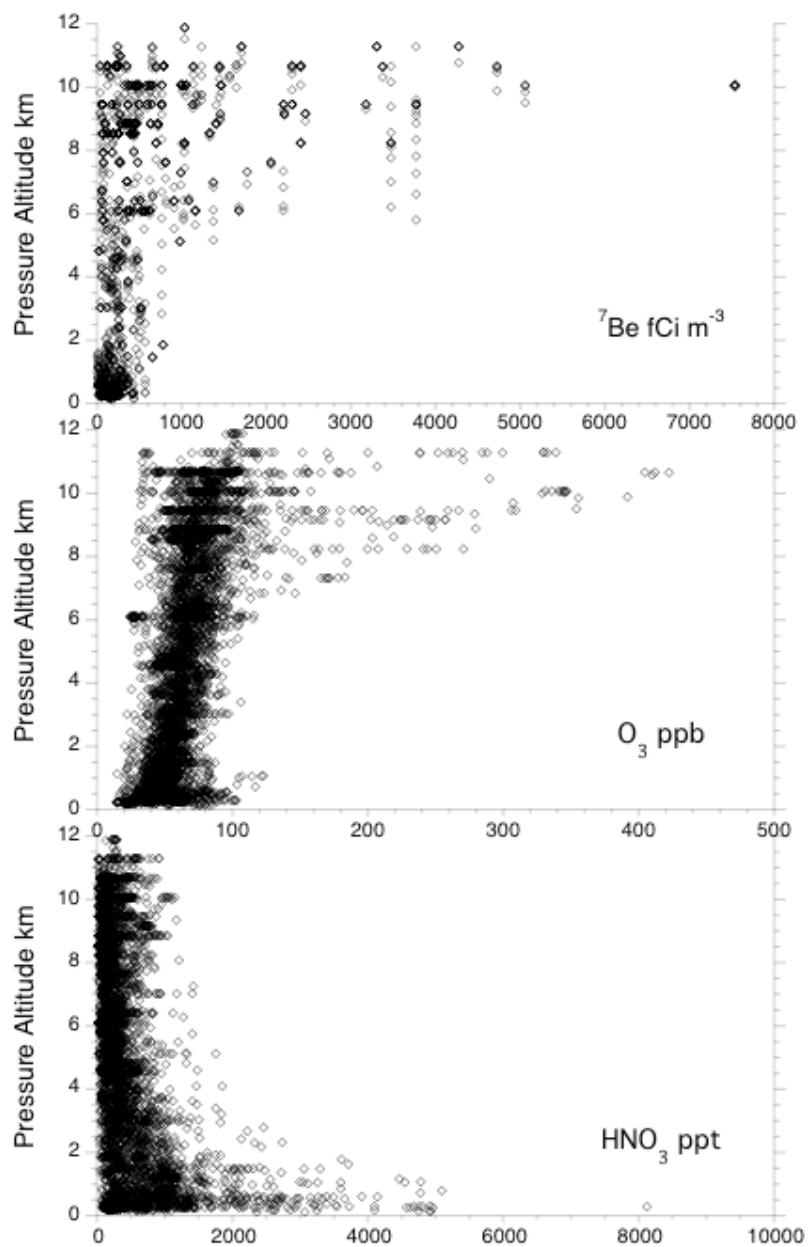


Figure 2. Altitude profiles of ${}^7\text{Be}$, O_3 , and HNO_3 from the DC-8 during INTEX A.

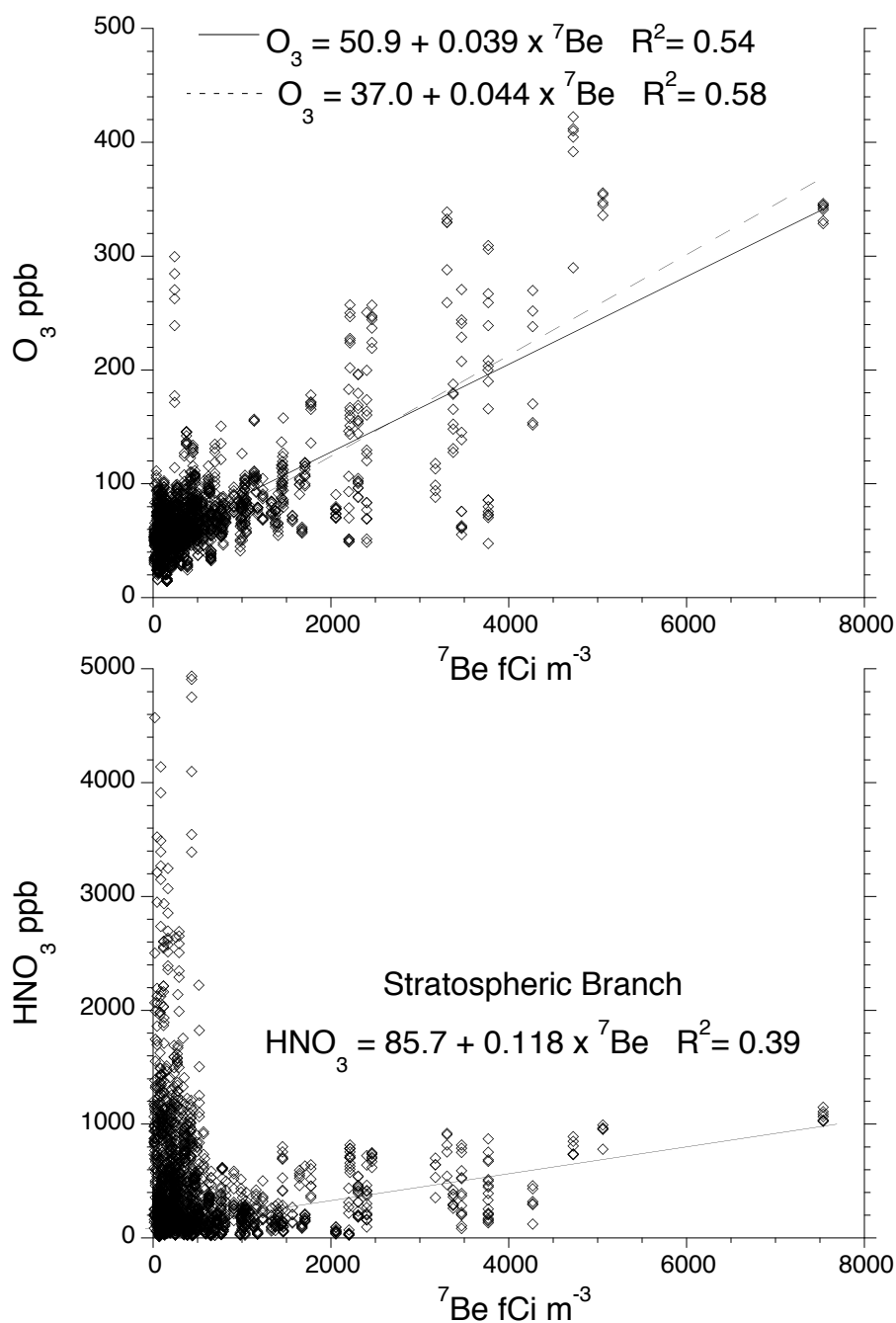


Figure 3. Scatter plots of O₃ (upper panel) and HNO₃ (lower panel) versus ⁷Be. The solid least squares regression line in the O₃ plot uses all data points, while the dotted line applies ⁷Be > 600 fCi as a filter. For HNO₃ the fit is only for the strongly stratospherically impacted samples (⁷Be > 600 fCi m⁻³). Note that one boundary layer sample with HNO₃ > 8 ppb is omitted from this plot for clarity.

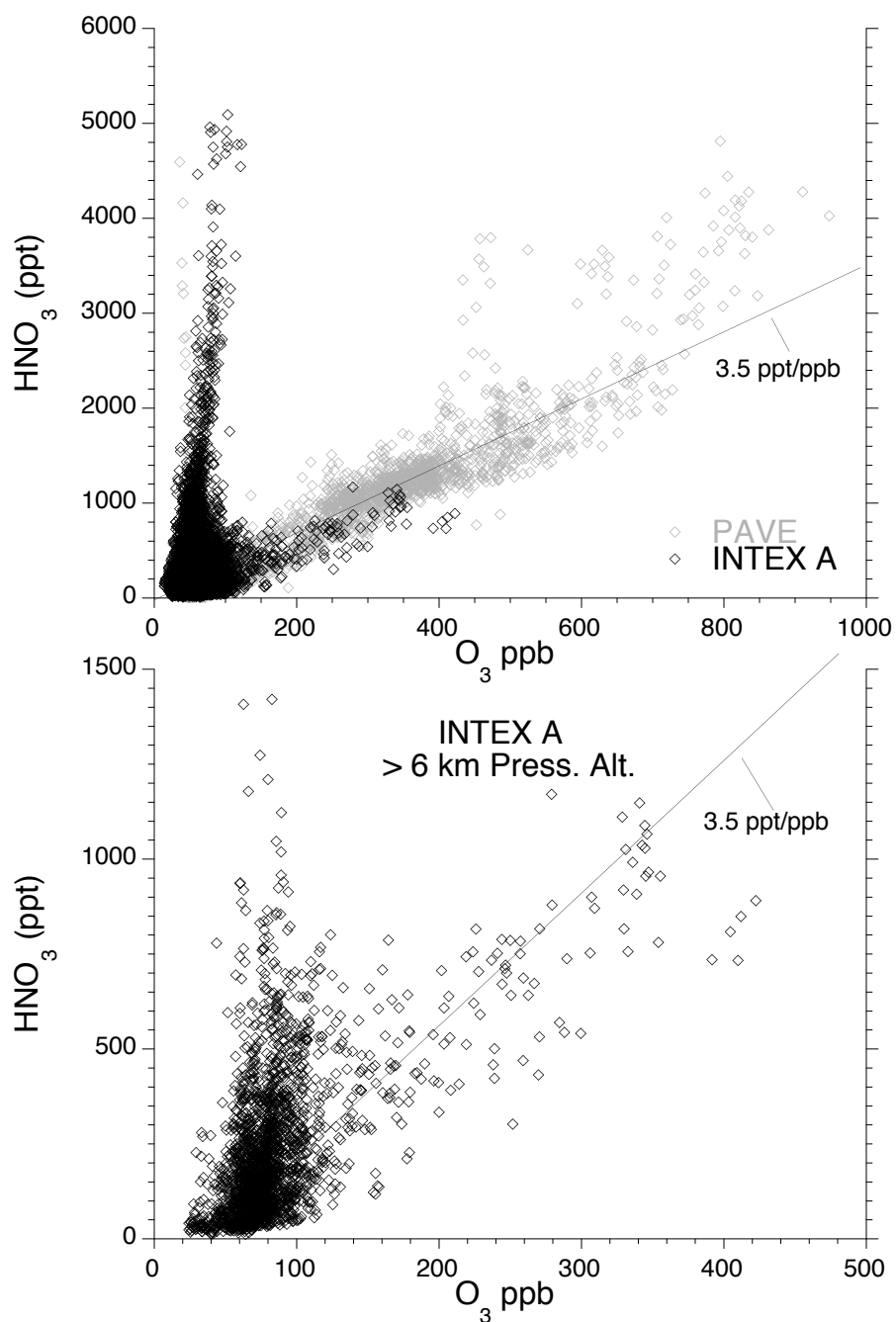


Figure 4. Nitric acid versus ozone. In the upper panel all data points from INTEX A are shown in black diamonds on top of PAVE data (grey diamonds). The ratio of 3.5 ppt HNO₃/ppb O₃ was characteristic of measurement in the lower stratosphere during PAVE (Dibb et al., 2006). In the lower panel INTEX A observations above 6 km are plotted on an expanded scale to focus on the upper troposphere. The line has a 3.5 ppt/ppb slope, but intersects the x axis at 40 ppb O₃.

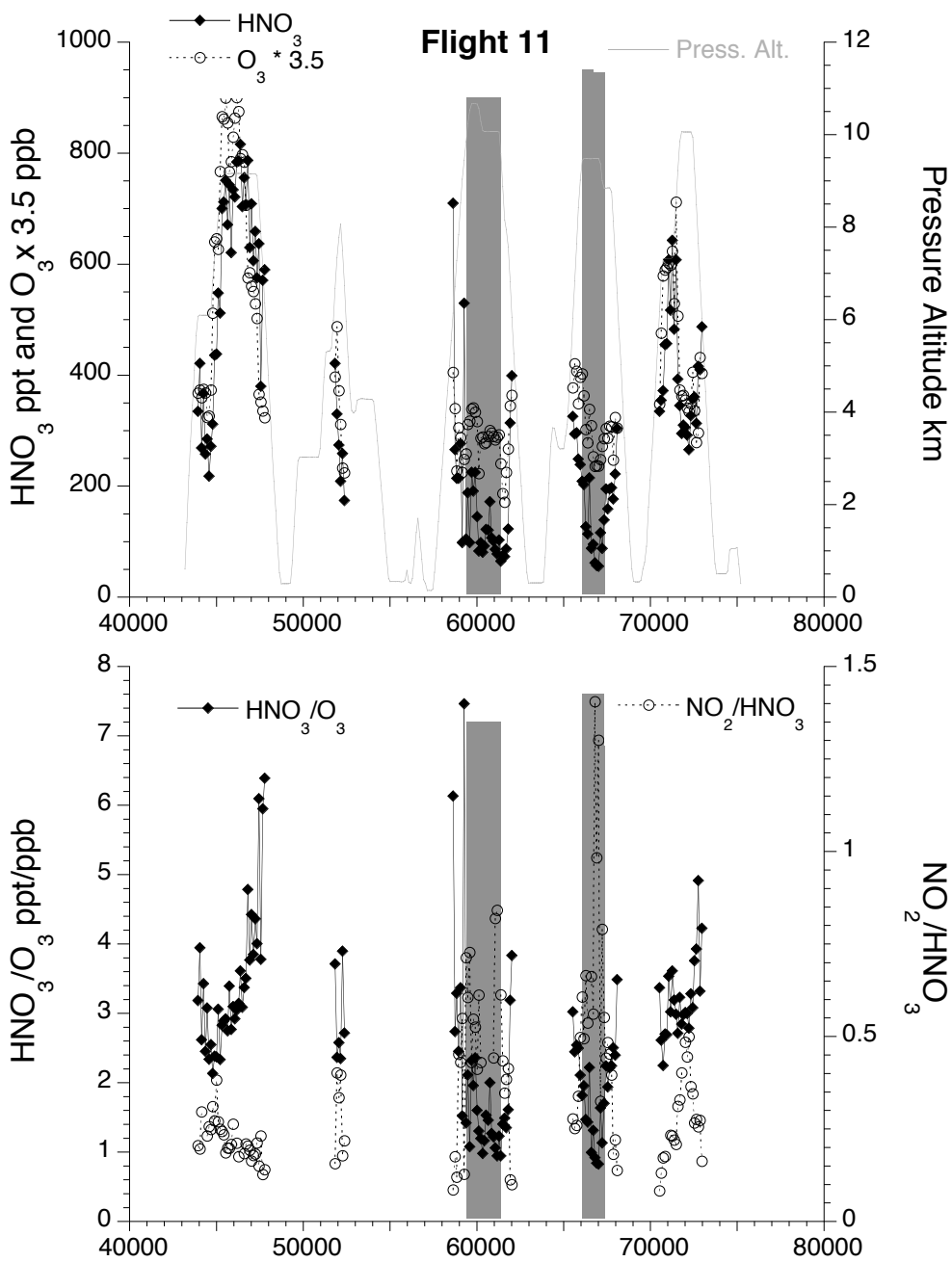


Figure 5. Example time series (from INTEX A flight 11) of the relationships between HNO₃, O₃, and NO₂ in the upper troposphere. Only samples collected above 6 km are shown, but upper panel depicts the DC-8 flight profile. Grey bars highlight intervals with enhanced NO₂ from convection (Bertram et al, this issue), increasing the NO₂/HNO₃ ratio and depressing the HNO₃/O₃ ratio (lower panel). The mixing ratios of HNO₃ and O₃ outside of these convectively influenced intervals covary rapidly, but their ratio stays near 3.5 most of the time.

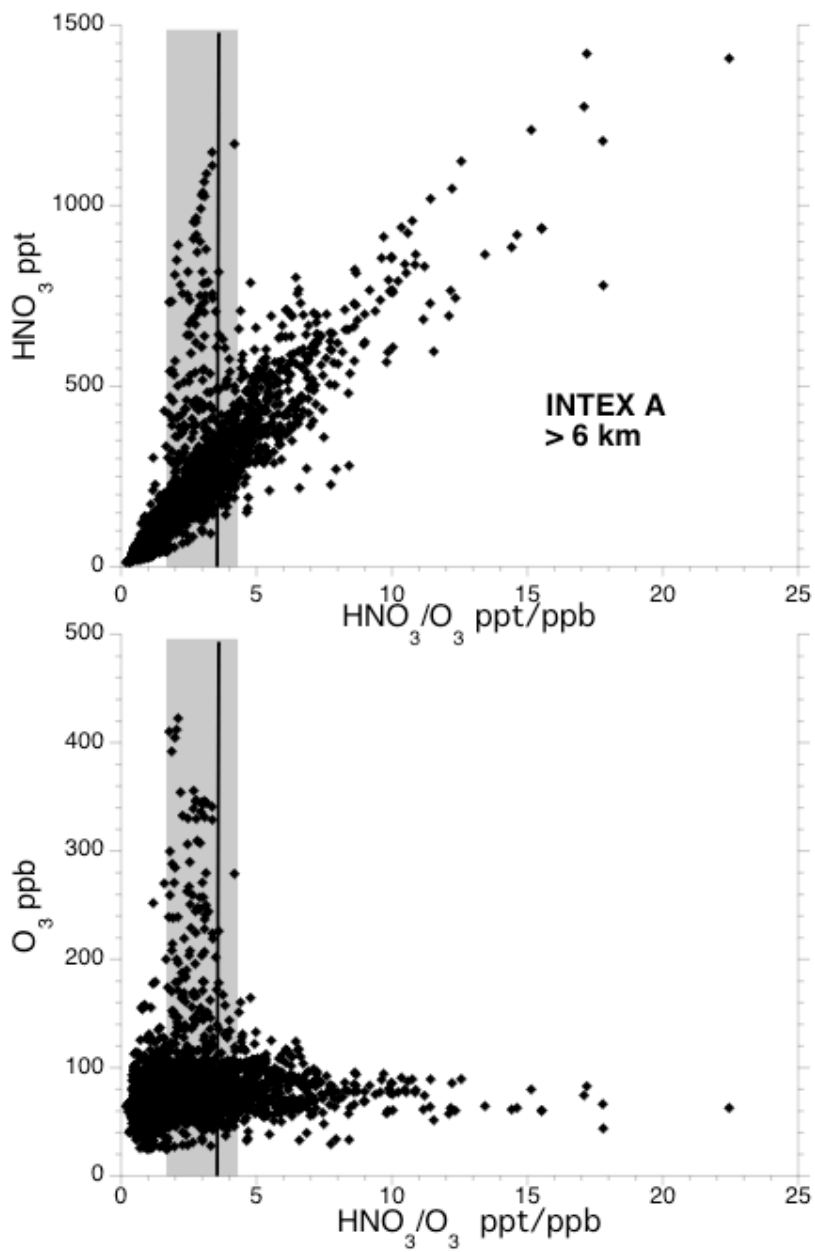


Figure 6. Nitric acid and ozone plotted against the HNO_3/O_3 ratio. Values of the ratio between 2.0 and 4.0 (grey shading) capture the stratospherically influenced HNO_3 and O_3 samples apparent in Figures 3 and 4. The stratospheric value of the HNO_3/O_3 ratio found during PAVE is shown by the vertical line.

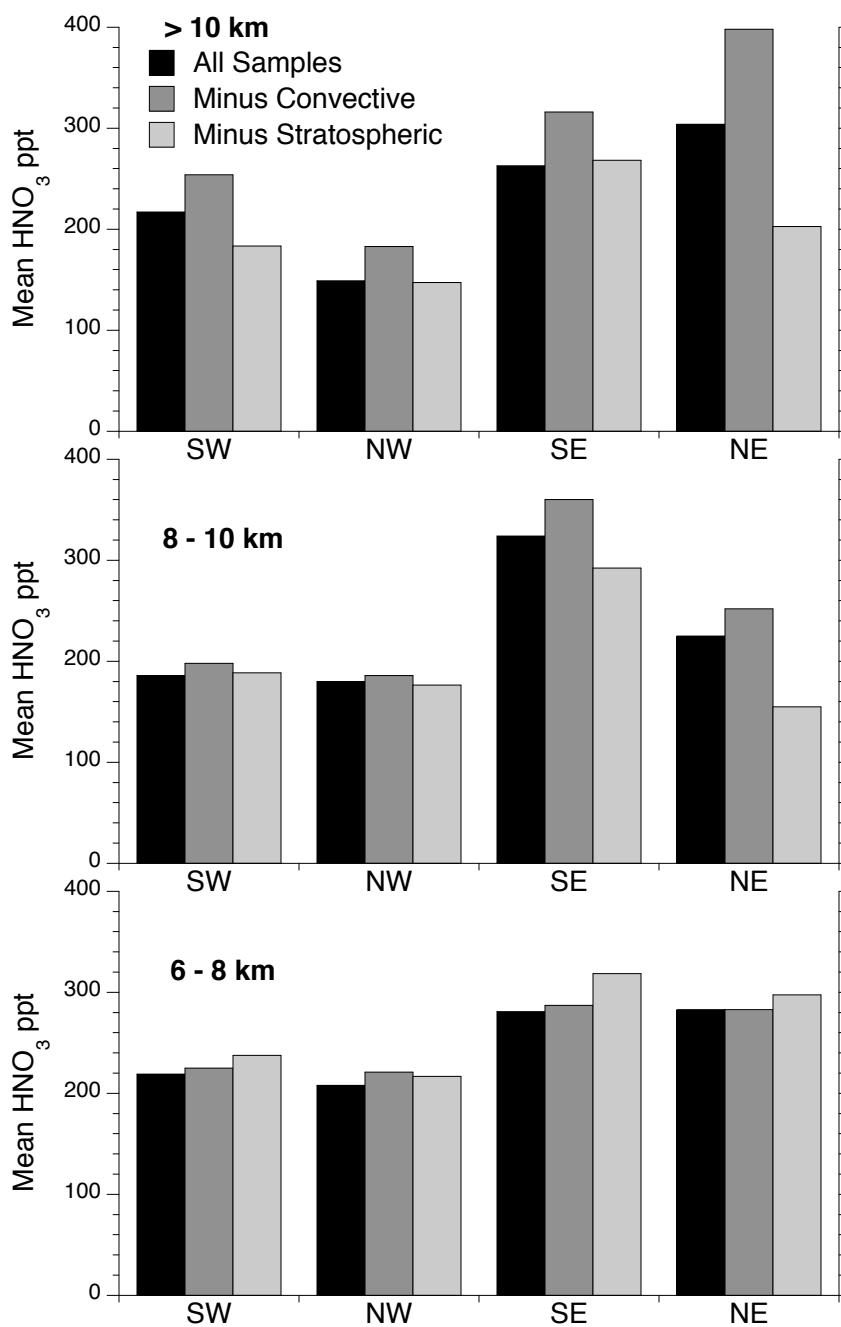


Figure 7. Mean HNO₃ mixing ratios in four geographic regions and three upper tropospheric altitude bins sampled by the DC-8 in INTEX A. Black bar includes all data, dark grey bars exclude samples with recent convective influence (NO₂/HNO₃ > 1.0) and the light grey bars exclude samples with stratospheric signature (2.0 < HNO₃/O₃ < 4.0).

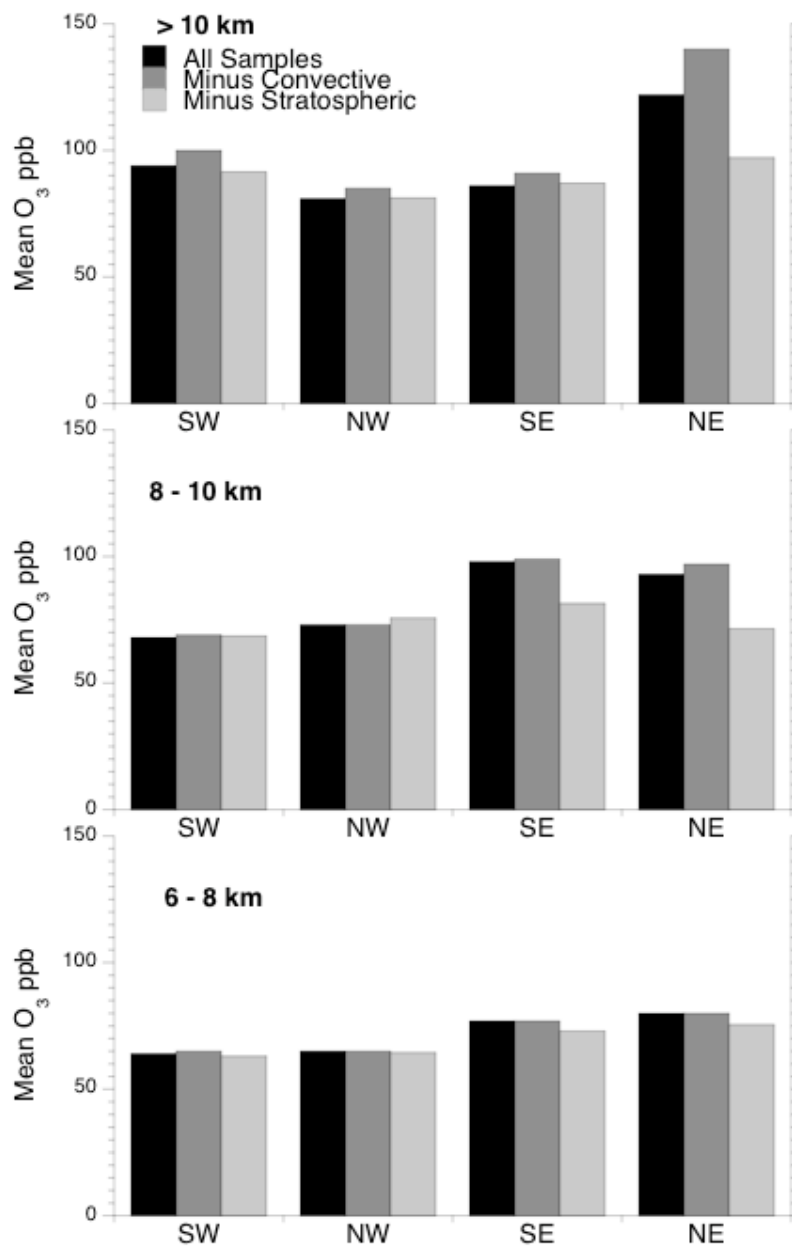


Figure 8. As in Figure 7, but for O₃.

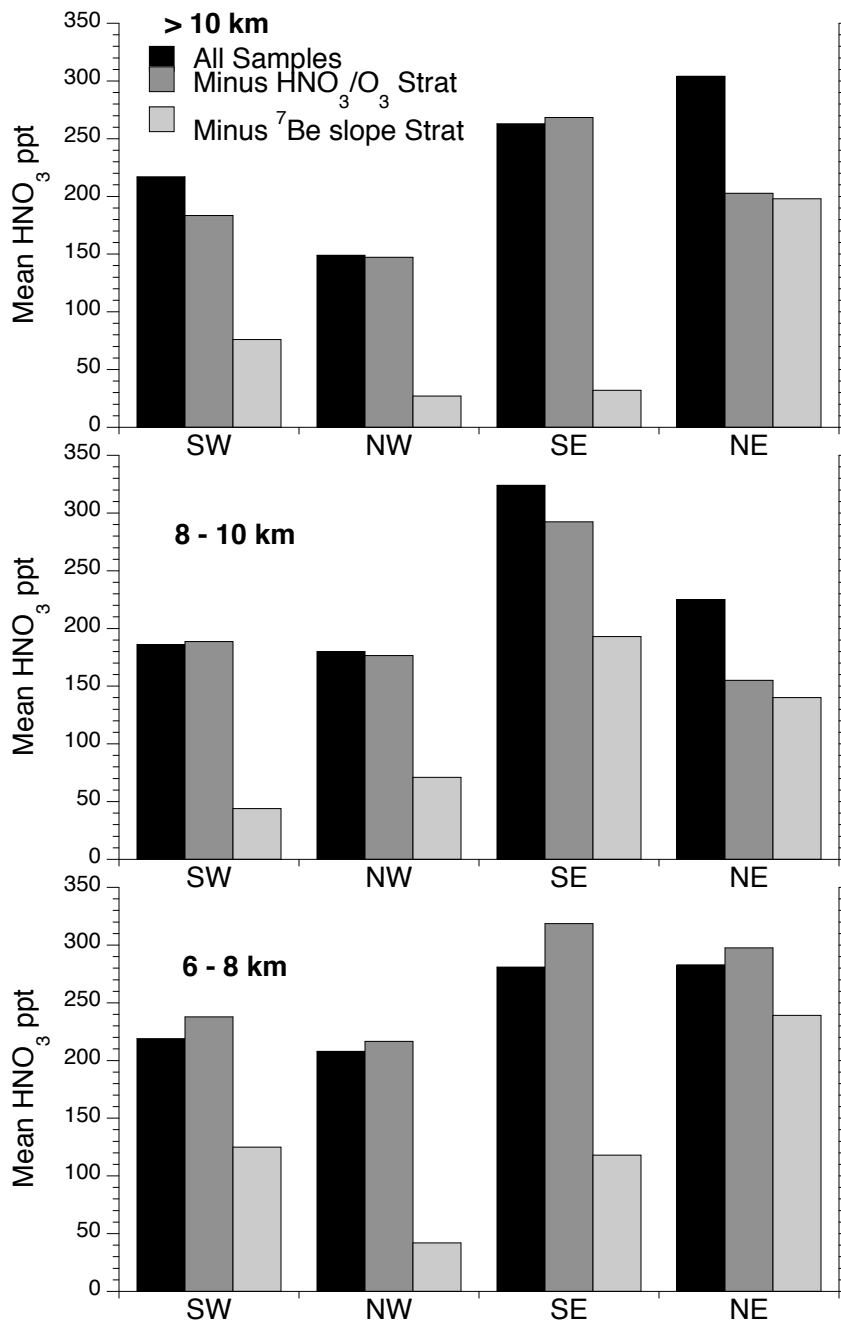


Figure 9. Comparison of the HNO₃/O₃ filter estimates of stratospheric influence (dark grey bars, same as “minus stratospheric” in Figure 7), and the modified estimate using just the slope of the correlation to ⁷Be (light grey bars, slopes from Figure 3).

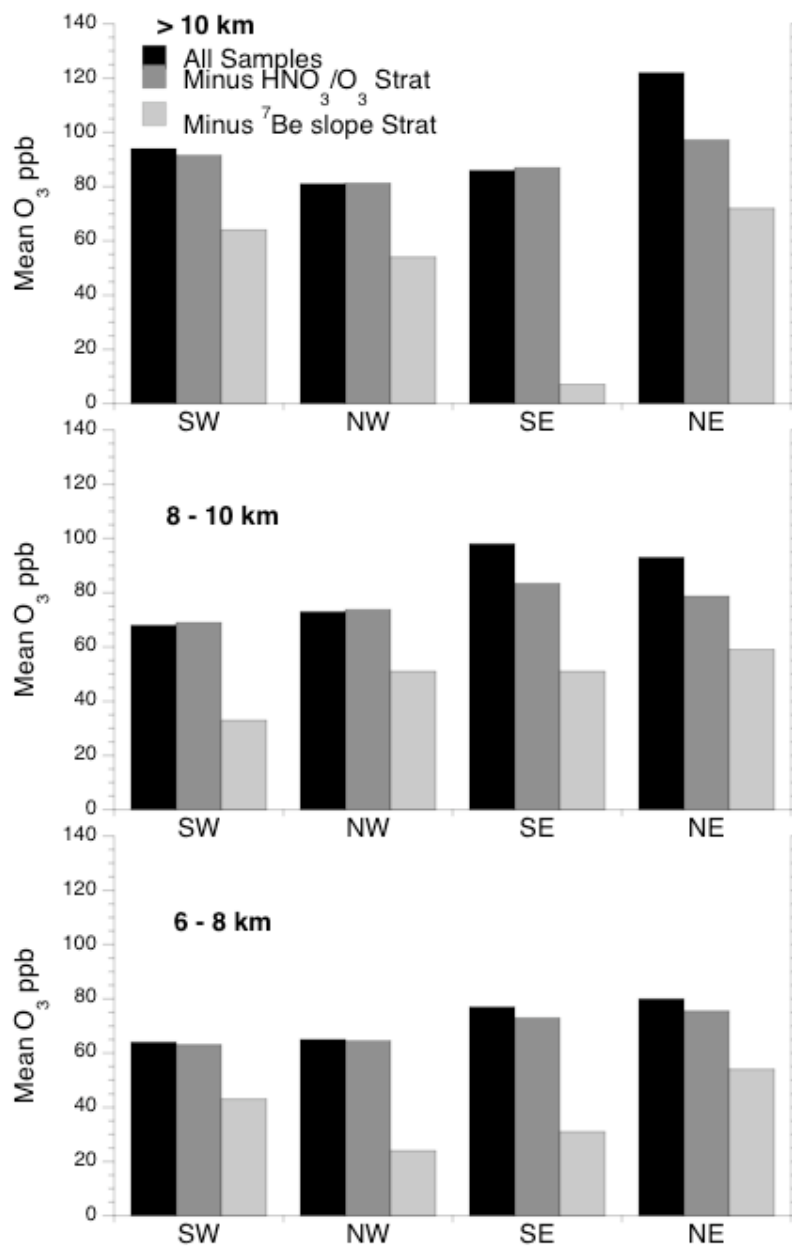


Figure 10. As in Figure 9, but for O₃. Dark grey bars are the same as in Figure 8.